Comparative genetic and demographic responses to climate change in three peatland butterflies in the Jura massif

Caroline Kebaïli[1,2], Stéphanie Sherpa[3], Maya Gueguen[1], Julien Renaud[1], Delphine Rioux[1], Laurence Després[1]

[1] Université Grenoble-Alpes, Université Savoie Mont Blanc, CNRS, Laboratoire d'Ecologie Alpine, F-38000, Grenoble, France

[2] Parc Naturel Régional du Haut-Jura, Lajoux, France

[3] Dipartimento di Scienze e Politiche Ambientali, Università degli Studi di Milano, I-20133, Milano, Italy

Credit authorship contribution statement

LD, SS and CK conceived the study; CK and DR performed the molecular work; JR and MG ran the SDMs; CK and SS performed the analyses and produced the Figures; CK, SS and LD wrote the manuscript. All authors made critical contributions and gave final approval for publication.

Acknowledgments

We thank Pierre Durlet, Jocelyn Claude, Perrine Jacquot, Frédéric Mora, Camille Barbaz, Luc Bettinelli, Marion Brunel and François Dehondt for initiating and coordinating this partenarial Academic-Wildlife Management project and for obtaining permits to collect from the French authorities (DREAL Auvergne Rhône Alpes), and all the collectors: Pierre Durlet, Axel Peyric (PNR Haut-Jura), Frédéric Mora, Perrine Jacquot, Catherine Duflo, Julien Ryelandt (CBNFC-

ORI), Jocelyn Claude, Romain Decoin, Anaëlle Bernard (Amis de la RNN du Lac de Remoray), Camille Barbaz, Michel Sauret (EPAGE Haut-Doubs Haute-Loue), Magalie Mazuy (CEN FC), and their respective structures. We also thank Christian Miquel for help in molecular work. CK was supported by a PhD fellowship from the Parc naturel régional du Haut-Jura the DREAL Bourgogne-Franche-Comté and ANRT (CIFRE grant number 2019/1732).

Abstract

Climate is a main driver of species distributions, but all species are not equally affected by climate change, and their differential responses to similar climatic constraints might dramatically affect the local species composition. In the context of climate warming, a better knowledge of the ability of dispersal-limited and habitat-specialist species to track climate change at local scale is urgently needed. Comparing the population genetic and demographic impacts of past climate cycles in multiple co-distributed species with similar ecological requirements help predicting the community-scale response to climate warming, but such comparative studies remain rare. Here, we studied the relationship between demographic history and past changes in spatial distribution of three protected peatland butterfly species (*Boloria aquilonaris*, *Coenonympha tullia*, *Lycaena helle*) in the Jura massif (France), using a genomic approach (ddRAD sequencing) and species distribution modeling (SDM). We found a similar and narrow thermal niche among species, and shared demographic histories of post-glacial decline and recent fragmentation of populations. Each species functions as a single metapopulation at the regional scale, with a North-South gradient of decreasing genetic diversity that fits the local dynamics of the ice cover over time. However, we found no correlation between changes in the quantity or the quality of suitable areas and changes in effective population size over time. This suggests that species ranges moved beyond the Jura massif during the less favorable climatic periods, and/or that habitat loss and deterioration are major drivers of the current dramatic decline observed in the three species. Our findings allow better understanding how history events and contemporary dynamics shape local biodiversity, providing valuable knowledge to identify appropriate conservation strategies.

Keywords: Comparative population genomics – Species distribution modeling – Genetic diversity – Demographic inference – Climate change – ddRAD sequencing

1. Introduction

Climate has major effects on the global distribution of species, but all species are not equally vulnerable to climate change. The variety of responses is the result of differences in species biology and ecology (dispersal behavior, niche characteristics and niche breadth, physiology, phenology) together with historical contingencies (Estrada et al., 2018; Pedreschi et al., 2019). For example, butterflies were shown to be more vulnerable to climate change than birds (Devictor et al., 2012) and within butterflies, habitat specialist species generally appear to be more at risk than generalist species (Warren et al., 2001; Settele et al., 2008; Heikkinen et al., 2010; Noreika et al., 2016). In fact, habitat specialization and sedentary behavior might have negatively affected the altitudinal shift response to recent past climate change among butterfly species (Habel et al., 2023). Furthermore, in contrast to several organisms that have already shown range shifts northwards as a response to ongoing climate warming (Parmesan et al., 1999; Devictor et al., 2012), southern populations of post-glacial relict species are often trapped in isolated altitudinal habitats (Turlure et al., 2010). Given the current rate of warming, we need to evaluate the ability of dispersal-limited and habitat specialist species to track their climate niches at local scale.

The population genetic and distributional responses of species to past climate changes can give insight on their capacity to cope with ongoing warming. The Pleistocene climatic fluctuations have profoundly impacted species distributions (Hewitt, 2000; Schmitt, 2007). During the last glacial maximum (LGM), many temperate species from Europe showed range contraction towards glacial refuges in Mediterranean peninsulas where the climate remained suitable (Taberlet et al., 1998; Hewitt, 2000, 2004). However, the picture is less clear for boreo-montane species (Schmitt and Varga, 2012). Some species may have survived the last glaciation in restricted non-glaciated areas at high latitude or altitude, or as small populations at the margin of the glaciated areas (Schoville et al., 2011; Sherpa et al., 2022). Other species may have

benefited from cold temperature and expanded their range during the LGM (Kebaïli et al., 2022). These different distributional responses of boreo-montane species are expected to result in distinct population demographic histories; for instance, a decrease in effective population size (Ne) during the LGM for species that remained within small ice-free refuges (Sherpa et al., 2022), or an increase in Ne for cold-adapted species that expanded during the LGM and reduced Ne during interglacial periods (Kebaïli et al., 2022). The current genetic diversity of populations should reflect, in part, their demographic and biogeographic history, with decreasing genetic diversity from the glacial refuge to the newly colonized areas (Hewitt 2004). However, very few studies have investigated the relationship between habitat suitability and demographic changes over time, and how currently co-distributed species with similar ecology did respond to past climate change.

The boreo-montane species *Boloria aquilonaris* (Nymphalidae, Heliconinae), *Coenonympha tullia* (Nymphalidae, Satyrinae) and *Lycaena helle* (Lycaenidae) have a patchy distribution in Europe and are among the most endangered European butterflies (van Swaay et al., 2011). The main causes of the recent decline of these peatland species are land-use changes (peat exploitation, drainage of wetlands and conversion to crop production or urbanization) and climate change (Settele et al., 2008; Noreika et al., 2016). The three species benefit from a high protection status both at the Europe and local scales, and a large amount of literature is available on their current distribution, local habitat requirements and population ecology through conservation monitoring programs (Settele et al., 2008; Turlure et al., 2010; Habel et al., 2011; Fisher et al., 2014; Weking et al., 2013, Noreika et al., 2016; Čelik et al., 2018; Lebigre et al., 2022; Osborne et al., 2022). Yet little is known about their evolutionary history and past distributions (but see Habel et al., 2010 for *L. helle*). Given that these peatland butterflies have a similar habitat, they might show an analogous demographic history of population decline concomitant with periods of habitat contraction. However, habitat quality rather than habitat

quantity might be a better predictor of local abundance, especially for habitat specialists such as peatland butterflies (Dennis and Eales, 1997; Noreika et al., 2016; Čelik et al., 2018; Lebigre et al., 2022). Furthermore, the three species differ in several life-history traits including larval host-plant, overwintering stages and microhabitat (Settele et al., 2008), which might result in slight differences in climatic niches and responses to climate change, and therefore in population histories.

Here, we ask whether habitat specialists such as peatland butterflies, which are co-distributed in the Jura massif but have distinct life-history traits, have a common demographic and biogeographic history in response to the climate changes during the last glacial cycle. Contrary to the Alps, the Jura massif has never been entirely covered by ice during the LGM (Lhosmot et al., 2022) and might have acted as a refuge for cold-adapted species, possibly in multiple distinct areas. This hypothesis has however hardly been tested so far (Sherpa et al., 2022). Combining fine-scale population genomics (Jura massif) and coarse-scale predictions of species distribution (Europe), we specifically address the following questions: (1) Do the three species present the same population genetic structure and a shared demographic history in the Jura massif? (2) Is their current distribution explained by the same climatic predictors? (3) How did the spatial distribution of favorable areas change over time for each species, and has the Jura massif always been a suitable area? (4) Is there a relationship between the effective population size and the quantity and/or the quality of climatically suitable areas in Europe and Jura since the last interglacial (LIG)?

2. Material and Methods

2.1 Studied species

In the Jura massif, the three species are univoltine and on-wing in May-June. They all are small butterflies with limited dispersal found in wetlands, but they differ in their larval-host plant,

overwintering stages and microhabitat. The Cranberry Fritillary *B. aquilonaris* is found in raised bogs (European Nature Information System (EUNIS) code: D1.1; https://www.eea.europa.eu/data-and-maps/data/eunis-habitat-classification-1) and wet heaths, in sheltered places at the edges of woods or in clearings. Eggs are laid on *Vaccinium oxycoccos*, the larval host-plant, but the caterpillar overwinters in the moss layer just after hatching and starts feeding only the following year: the summer thermal buffering of the *Sphagnum* hummocks appear to be as important as the presence of the host plant for larval survival (Settele et al., 2008; Turlure et al., 2010). The Violet Copper *L. helle* lives in moist or wet eutrophic and mesotrophic grasslands (EUNIS code: 3.4) and uses *Bistorta officinalis* as larval foodplant, and overwinters as a pupa (Habel et al., 2011; Fisher et al., 2014). *Lycaena helle* dispersal is limited by both forests and fully open habitats as this butterfly prefers wind-sheltered stands (Fischer et al., 1999; Bauerfeind et al., 2009; Chuluunbaatar et al., 2009; Lebigre, 2022). The Large Heath *C. tullia* is a specialist of good-quality lowland fens with water table at or just below the surface (Lebigre et al., 2022), typically found in poor fens and soft-water spring mires (EUNIS code: D2.2). Unlike the two other species, the caterpillar can feed on many different grasses (Clarke, 2022) but it feeds on *Carex* sp. in limestone Jura Mountains (Decoin et al., 2021). The third instar caterpillars hibernate in the tussocks of the foodplant and actively escape from flooding by climbing up so that winter vegetation structure is a major constrain for this species (Joy and Pullin, 1997; Weking et al., 2013; Čelik et al., 2018; Osborne et al., 2022).

2.2 Study area and sample collection

The study area covers the Jura massif, on the border between France and Switzerland (Figure 1). Sampling localities were distributed into three main geographical regions in France: Haut-Jura (HJ); Doubs and Drugeon valleys (DDV); plateau of Russey (RUS) (Figure 1; Supplementary Table S1). The sampling was performed by qualified personnel from:

Conservatoire Botanique Nationale de Franche-Comté – Observatoire des Invertébrés (CBNFC–ORI); Conservatoire d'Espaces Naturels de Franche-Comté (CEN FC); Réserve Naturelle du Lac de Remoray; Établissement Public d'Aménagement et de Gestion de l'Eau Haut-Doubs Haute-Loue (EPAGE HDHL); Parc naturel régional du Haut-Jura (PNRHJ). The experimental protocols were validated by the French authorities (authorization number: DDPP01-21-052) and by the Swiss Canton of Vaud authorities (authorization number: 2021-3539). For each locality, one to nine butterflies were captured using hand-nets, and one hind leg was collected before immediate release. This method was shown to cause low disturbance on post-release flight behavior and survival in butterflies (Koscinski et al., 2011), thus minimizing the impact of sampling on vulnerable populations of protected species. We sampled 52 individuals from 11 localities for *B. aquilonaris*, 100 individuals from 18 localities for *C. tullia* and 236 individuals from 67 localities for *L. helle*. For *L. helle*, two additional localities were sampled in the Canton de Vaud, Switzerland (Supplementary Table S1). The sampling was performed during the flight period in 2018, 2020 and 2021. Collected tissues were stored at -20°C until DNA extraction.

2.3 DNA extraction and ddRAD-seq libraries preparation

DNA was extracted (DNEasy Blood & Tissue kit, Qiagen) and 50 ng was double-digested with *SbfI*-HF and *MspI* restriction enzymes (New England Biolabs) and individually tagged during ligation to P1 and P2 adapters as described in Kebaïli et al. (2021). After a first purification step with 1.5 volumes of NucleoMag NGS Clean-up and Size Selected (Macherey-Nagel SAS), the adapters-ligated DNA fragments were size-selected for a length of 200–600 bp (Pippin-Prep 2% gel cassette; Sage Science Inc). Libraries were amplified in 10 independent replicates, which were pooled and purified with 1 volume of NucleoMag NGS Clean-up and Size Selected (Macherey-Nagel SAS) (see Kebaïli et al., 2022 for PCR conditions). The libraries were

sequenced on Illumina HiSeq 2500 (2 × 125bp) in 2018 and Illumina NovaSeq 6000 (2 × 150bp) in 2020 and 2021.

2.4 Genomic data treatment

After trimming adapters (BBDuk from the BBTools package; Bushnell, 2014), the assembly of ddRAD loci and SNP calling were performed using the Stacks v2.2 *de novo* pipeline (Rochette et al., 2019). Reads were demultiplexed, filtered based on quality and cut to 110bp (*process_radtags*). Loci reconstruction was performed for each species separately, using a maximum of eight mismatches to merge two stacks into a polymorphic locus within an individual (*ustacks*) and between individuals (*cstacks*). Single-end catalog loci (*sstacks*) were merged into single loci (*gstacks*) and SNP datasets included all biallelic variant positions (*populations*).

SNPs were filtered using VCFtools v1.16 (Danecek et al., 2011), following a modified approach of the one proposed by O'Leary et al. (2018). We removed SNPs with read coverage ≤ 5X and mean read coverage among individuals ≤ 15X. To minimize the amount of missing data in final datasets (< 15%), we discarded individuals with high percentage of missing data: six for *B. aquilonaris*; thirteen for *C. tullia*; eighteen for *L. helle* (Supplementary Table S2). To maximize the number of SNPs, we applied different filtering parameters for each species, retaining SNPs with < 30% missing data for *C. tullia* and *L. helle*, and SNPs with < 50% missing data for *B. aquilonaris*. Finally, we retained one random SNP per locus.

2.5 Genetic diversity and population structure

Population genetic structure and diversity analyses were performed after filtering the SNP datasets for low frequency variants (minor allele frequency, MAF ≤ 1%). We first inferred individual ancestry coefficients using the program ADMIXTURE v1.3 (Alexander et al., 2009).

The optimal number of K genetic clusters was determined based on the lowest error rate from a 10-fold cross-validation (CVE). To evaluate the level of genetic differentiation between sampling localities, we calculated pairwise F_{ST} using the *hierfstat* package v0.5-10 (Goudet, 2005) in R (R Core Team, 2022).

The *hierfstat* R package was also used to calculate population genetic diversity, including observed heterozygosity (Ho), expected heterozygosity (He), inbreeding coefficient (F_{IS}), and differentiation between a given locality and all the localities in the study area (population-specific F_{ST}). For Ho, He and F_{IS}, 95% confidence intervals (CI95) were estimated from 1,000 bootstraps of the data, and 100 bootstraps for the population-specific F_{ST}. Spatial patterns of genetic diversity were inferred using the program EEMS (Petkova et al., 2016). We computed genetic dissimilarities on a spatial grid of 600 demes for each species. The analysis was repeated independently three times, with 4,000,000 MCMC iterations, a burn-in of 1,000,000 and a thinning interval of 10,000. The average posterior distributions of within-deme genetic variability were represented on maps using the *rEEMSplots* R package (Petkova et al., 2016).

2.6 Climate niche models

To determine the best climatic predictors of the distribution of each of the three species at the European scale, we performed species distribution models (SDMs) using the *biomod2* R package v4.2.2 (Thuiller et al., 2016). Species presences were extracted from the Global Biodiversity Information Facility database (GBIF, 2022). We selected human observations after 1970 with coordinate precision < 5 km. We added the geo-reference of all our sampling localities (Supplementary Table S1) and of local managers population monitoring data recorded after 1970. In total, we obtained 11,432 occurrences for *B. aquilonaris*, 16,106 for *C. tullia* and 4,932 for *L. helle*. To reduce sampling bias, one occurrence was randomly selected within a

raster cell of 1 km (Fourcade et al., 2014), resulting in 2,944, 1,515 and 603 occurrences, respectively. We selected six bioclimatic variables for 1970–2000 from the WorldClim database v2.1 (2.5 arc-minutes; Fick and Hijmans, 2017) that were shown to be important predictors for another co-distributed butterfly (Sherpa et al., 2022): mean annual temperature (BIO1); mean diurnal range (BIO2); isothermality (BIO3); mean temperature of the wettest quarter (BIO8); annual precipitation (BIO12); precipitation seasonality (BIO15).

SDMs included five statistical models: generalized linear (GLM), additive (GAM), and boosting (GBM) models; maximum entropy (MAXENT); random forest (RF) (Araùjo and New, 2007; Marmion et al., 2009). A dataset of 10,000 random pseudo-absences was produced using a surface range envelope model. Training data included 70% of the occurrences randomly sampled, and the remaining 30% were used to evaluate model performance with two metrics: the true skill statistic (TSS) and the area under the curve (AUC). We performed a three-fold internal cross-validation, resulting in a total of 45 models that were merged using the weighted sum of probabilities (EMwmeanByTSS) or the committee averaging (EMcaByTSS) methods. For each bioclimatic variable, we calculated the importance of its contribution to the model (see Thuiller et al., 2009) and variable importance was normalized to the model for comparison among species.

2.7 Demographic inferences

Changes in effective population size (Ne) over time were inferred using the Stairway Plot method v2 (Liu and Fu, 2020) based on the site frequency spectrum (SFS). The SFS was calculated from all SNP positions (no filter on MAF) and imputed genotypes. Missing data was imputed to the most likely genotype using the LEA R package v3.0.0 (*impute* function; Frichot et al., 2014), and a number of ancestral populations corresponding to the number of geographical areas: N = 5 for *B. aquilonaris* and *C. tullia*; N = 8 for *L. helle* (Supplementary

Table S1). We used a mutation rate of 2.10^{-9} based on previous studies in butterflies (Keightley et al., 2015; Kebaili et al., 2022; Sherpa et al., 2022) and a generation time of one year, all species being univoltine. The total sequence length accounted for both polymorphic and monomorphic loci. Two-epoch models were built with 67% of segregating sites used for training and break points following authors' recommendation. Median estimates of Ne and CI95 were obtained from 200 bootstrap replicates. Stairway Plot analyses were carried out at: (1) the population level based on population genetics results; (2) the species level including all 48 individuals for *B. aquilonaris* and down-sampling randomly the *C. tullia* and *L. helle* datasets to the same sample size.

Divergence times between the three main geographical areas (HJ, DDV, and RUS) were inferred using DIYABC v2.1.0 (Cornuet et al., 2014), using the SNP datasets of 48 individuals filtered for MAF ≤ 1%. Two series of analyses determined the time period and mode of divergence. The first analyses compared three scenarios of synchronous divergence: (1) during an ancient decrease in Ne (Split-1D); (2) during a recent decrease in Ne (Split-2D); (3) during an ancient increase in Ne (Split-Exp) (Supplementary Table S3). The second analyses compared: (1) synchronous divergence times (Synch-Split); (2) an early divergence of RUS followed by HJ and DDV (Asynch-Split1); (3) an early divergence of HJ followed by RUS and DDV (Asynch-Split2) (Supplementary Table S3). We ran 100,000 simulations for each scenario, using the mean genetic diversities within populations, F_{ST} and Nei's distances among populations as summary statistics. The 1% of simulated data closest to the observed data were used to calculate the posterior probabilities of scenarios (logistic regression) and the posterior distribution of demographic parameters. Confidence in scenario choice (Type I and Type II errors) was evaluated from 100 newly simulated datasets.

2.8 Changes in potential distribution and species demography over time

To characterize the changes in species potential distribution over time, we projected SDMs into current climate (1970–2000) and eight palaeoclimates: Late Holocene (LatH: 0.3–4.2 kya); Mid Holocene (MidH: 4.2–8.3 kya); Early Holocene (EarH: 8.3–11.7 kya); Younger Dryas Stadial (YDS: 11.7–12.9 kya); Bølling-Allerød (BA: 12.9–14.7 kya); Heinrich Stadial 1 (HS: 14.7–17.0 kya); Last Glacial Maximum (LGM: ca. 21 kya); Last Interglacial (LIG: ca. 130 kya). Palaeoclimate data was retrieved from the PaleoClim database (2.5 arc-minutes; Brown et al., 2018; Karger et al., 2020). Palaeoclimate projections were resampled to a 1×1 km resolution, using the k-nearest neighbors method in QGIS v3.22.3 (QGIS Development Team, 2022).

The availability of suitable habitats at each of the nine time periods was characterized by two metrics. First, we calculated the average predicted probability of presence (pp) across all cells (hereinafter habitat quality). Second, we used the pp threshold that maximizes the TSS score (ppTSS) for each species model and calculated the total area with predicted presence: pp > ppTSS (hereinafter habitat quantity). These two metrics were calculated at the European scale as well as at the scale of the Jura massif, by working on the geographic subset of SDM projections corresponding to the massif. Raster manipulation and indices were calculated using QGIS. To evaluate the impact of past climate fluctuations on the species demography history, we combined our results of climate niche and demographic models. We tested the relationship between changes in habitat quality and habitat quantity over time, and changes in Ne over time. For a given time period, the Ne corresponded to the mean of the inferred median Ne in this period based on species demographic history (all populations combined) using the Stairway Plot method. The relationships between Ne and habitat metrics, both at European and Jura massif scales, were tested using Spearman correlations in R.

3. Results

3.1 Genetic datasets

We obtained an average of 0.46 ± 0.28 (SD; standard deviation) million reads per individual for *B. aquilonaris* (Ba), 0.56 ± 0.46 million reads for *C. tullia* (Ct) and 0.78 ± 0.79 million reads for *L. helle* (Lh) after quality filtering (Supplementary Table S2). After dropping individuals with a high proportion of missing data, the final sample sizes (N) for the three species were N_{Ba} = 48, N_{Ct} = 87 and N_{Lh} = 218. After applying the missing data and physical linkage filters, the number of loci was 380 for *B. aquilonaris*, 1,305 for *C. tullia* and 1,569 for *L. helle*, which were used for Stairway Plot analyses. After filtering for low frequency variants, the datasets included 380 SNPs for *B. aquilonaris*, 1,293 SNPs for *C. tullia* and 1,455 SNPs for *L. helle*, which were used for population structure and diversity analyses, and divergence time estimations (DIYABC). The average percentage of missing data among individuals per locus was 10.76 ± 7.97 for *B. aquilonaris*, 12.44 ± 8.85 for *C. tullia* and 11.78 ± 7.77 for *L. helle* (Supplementary Table S2).

3.2 Population genetic structure and diversity

The level of population differentiation in the Jura massif varied among species. The optimal number of genetic clusters from ADMIXTURE analysis was K = 1 for *B. aquilonaris* and *C. tullia*, and K = 3 for *L. helle* (Supplementary Figure S1). Investigating higher values of K did not reveal a clear geographic structuring for *B. aquilonaris* (Figure 3; Supplementary Figure S2). For K = 3 genetic groups, the two southern localities of the HJ region (mainly dark red cluster) differentiated from the four northern localities of the RUS region (mainly orange cluster). However, most localities showed a high number of admixed individuals. For *C. tullia*, all localities in the RUS region showed genetic differentiation with those of the HJ and DDV regions for K = 2, and these two last regions were further separated for K = 3 (Figure 3; Supplementary Figure S3). For *L. helle*, the optimal number of K = 3 groups revealed population structure largely corresponding to the three geographical regions but with substantial

admixture (Figure 3; Supplementary Figure S4). Increasing K up to 6 further separated localities from the HJ and DDV regions according to their geography, with three areas in HJ: southern HJ, Northern HJ and Grandvaux-Malvaux; two areas in DDV: Haut-Doubs and Drugeon basin (Figure 3; Supplementary Table S1).

The three regions exhibited different spatial patterns of genetic diversity. The HJ region was the less genetically diversified in all the three species, and the RUS region had the highest diversity for *B. aquilonaris* and *C. tullia* but it was the DDV region for *L. helle* (Figure 2A; Table1). In accordance, significant spatial genetic dissimilarities were detected for *B. aquilonaris* and *C. tullia*, with a decreasing gradient of diversity from North to South, whereas *L. helle* rather showed a diverse population in the center of the study area and a reduction of diversity at extreme North and South localities (Figure 2B).

For most regions, the distribution of heterozygosity (observed, Ho; expected, He) was bimodal, indicating two groups of localities: a group with a high genetic diversity and a group with a lower genetic diversity (Figure 2A). This pattern is typical of a metapopulation system, with some well-connected and highly diversified localities corresponding to the core (or source) population, and more isolated (sink) populations suffering from drift and genetic erosion. Accordingly, population-specific F_{ST} were significantly positive (indicative of the effect of genetic drift) for all localities in all regions but lower in the most diverse regions for *C. tullia* (RUS) and for *L. helle* (DDV) (Table 1). Another indication of a dynamic, non-equilibrium, metapopulation functioning in the three species is the significantly positive inbreeding coefficient F_{IS} observed in all localities, which is especially high in *C. tullia* (Table 1). The average pairwise F_{ST} among localities within regions revealed spatial variation in the level of population differentiation. In *B. aquilonaris*, the most diversified RUS region showed the lowest genetic differentiation among localities ($F_{ST} = 0.085 \pm 0.05$) compared to differentiation within HJ ($F_{ST} = 0.227 \pm 0.04$) and within DDV ($F_{ST} = 0.199 \pm 0.03$) (Supplementary Table

S5). For the two other species, the localities within the DDV region were the less differentiated, with an average pairwise $F_{ST} = 0.067 \pm 0.04$ compared to the HJ ($F_{ST} = 0.111 \pm 0.07$) and RUS ($F_{ST} = 0.116 \pm 0.06$) regions in *C. tullia* and $F_{ST} = 0.048 \pm 0.04$ compared to the HJ ($F_{ST} = 0.116 \pm 0.06$) and RUS ($F_{ST} = 0.096 \pm 0.08$) in *L. helle* (Supplementary Tables S6 and S7).

3.3 Species demographic history

The demographic history of populations in the Jura massif revealed consistent patterns among the three regions and for the three species (Supplementary Figure S5). Given the metapopulation functioning of each species suggested by population structure and diversity analyses, we inferred the changes in effective population size (Ne) over time at the species level including individuals from all the three regions (Figure 4A). Two species (*C. tullia* and *L. helle*) showed an ancient demographic expansion, with an increase in Ne between 1 Mya and 200 kya. All species showed a relatively recent decrease in Ne, which started during the last glacial period (approximately 25 kya) for *B. aquilonaris* and *L. helle*, and more recently (6 kya) for *C. tullia*.

The three species showed similar time and mode of divergence between regions in the Jura massif (Figure 4B). For the first DIYABC analysis testing the period of divergence (ancient vs. recent), the most likely scenario was a recent split between the HJ, RUS and DDV regions (scenario Split-2D; Table 2). For the second DIYABC analysis testing the mode of divergence (synchronous vs. asynchronous), the most likely scenario was a first divergence of the RUS region, followed by the divergence between the southern regions DDV and HJ (scenario Asynch-Split2; Table 2). The first population split (S1) occurred during Mid Holocene (7.0 kya) for *C. tullia* and *L. helle* and more recently during Late Holocene (2.1 kya) for *B. aquilonaris* (Figures 4C; Supplementary Table S8). The second split (S2) was estimated during the Late Holocene, approximately 1.4 kya, 0.8 kya and 2.6 kya for *B. aquilonaris*, *C. tullia* and

L. helle, respectively. While the S1 split is subsequent to the ancient decrease (D1) in Ne in the ancestral populations (no overlap between S1 and D1), the S2 split occurred at the same time as the more recent decrease (D2) in Ne (overlap between S2, D2R and D2HD).

3.4 Species current climate distribution

Species distribution model (SDM) evaluation statistics revealed a good performance of all models on average for *B. aquilonaris* (TSS = 0.72; AUC = 0.94), *C. tullia* (TSS = 0.85; AUC = 0.98) and *L. helle* (TSS = 0.82; AUC = 0.97). The main climatic predictor of the current distribution of the three species was the mean annual temperature (BIO1; > 40%, Table 3). At the European scale, the thermal niche of the three species was extremely narrow and at their highest limit in the Jura massif (Table 3), *L. helle* being the most narrow-range and thermophilic species with a BIO1 range excluding negative temperatures. Isothermality (BIO3) and precipitation seasonality (BIO15) were also two important predictors of the three species distribution, while total annual precipitation (BIO12) was the least important predictor. SDMs further revealed differences in climatic preferences between the three species. Temperature of the wettest quarter (BIO8) was important only for *B. aquilonaris* and *C. tullia*, and diurnal range (BIO2) only for *C. tullia* (Table 3).

SDM projections under current climate conditions revealed the largest predicted distribution in Western Europe for *B. aquilonaris* (1,426,977 km), mainly in Scandinavia (Figure 5A). Its southern potential distribution was more fragmented on plateaus and mountains including very isolated patches. The two other species had a more restricted distribution. Climatically suitable areas for *C. tullia* (581,681 km) were mainly located in Northern Europe, the UK, as well as few patches in the Alps and the Jura massif (Figure 5B). The last species *L. helle* (325,135 km) had the smallest Scandinavian distribution, but encountered suitable areas in most of southern mountain ranges (Figure 5C). In the Jura massif, *B. aquilonaris* and *L. helle*

had similar predicted distributions composed of a large suitable area in high altitudes (> 900 masl), with a potential distribution range of 8,418 km and 7,466 km , respectively (Figures 5D and 5E). The predicted distribution range of *C. tullia* was reduced to 2,106 km at altitudes <900m (Figure 5F).

3.5 Species past climate distribution

SDM projections under the eight paleoclimates revealed similar responses among the three species at the European scale (Figure 6A; Supplementary Figures S6 to S8). During the LIG, the distribution of climatically suitable areas included northern Europe and mountain chains, with a larger predicted distribution for *C. tullia* and *B. aquilonaris* than for *L. helle*. During the LGM, the projected distributions predicted an increase in habitat quantity for all species compared to LIG, but an increase in habitat quality only for *B. aquilonaris* and *L. helle*. This predicted geographic expansion was associated with a cooling of the climate and high values of isothermality overlapping well the species temperature requirements (Figure 6A). After the LGM, the quantity of habitats strongly decreased for all species, especially for *C. tullia* and *L. helle* whereas suitable habitats for *B. aquilonaris* were more abundant. Predicted habitat quality and quantity slightly increased since the late Holocene.

The changes in the quality and the quantity of habitats over time in the Jura massif were completely different from those observed at the European scale, with a decrease between LIG and HS similarly for the three species when the ice sheet covered a large area (Figure 6B). The changes in the distribution of climatically suitable areas over time were relatively similar for *B. aquilonaris* and *L. helle* (Figures 5D and 5F). During the LGM, the South of the Jura massif was covered by ice, which restricted the suitable areas for *B. aquilonaris* and *L. helle* in lowlands to the North of the massif. This LGM reduction of the distribution range was even more dramatic for *C. tullia*, with suitable areas only in the West of the massif (Figure 5E). Since

the HS period, the warming of the climate and ice retreat created new suitable habitats for *B. aquilonaris* and *L. helle*, which remained nearly constant until present days (Figures 5D, 5F and 6A). However, the projected distributions suggested an absence of suitable habitats for *C. tullia* in the Jura from the HS until the Mid Holocene (Figures 5E and 6A).

3.6 Effect of past climate changes on species demographic history

Our assessment of the impact of past climate fluctuations on the effective population size of peatland butterflies currently found in the Jura massif revealed two contrasting patterns between habitat quantity and quality. All the Spearman correlation tests between changes in the quantity of suitable habitats and Ne over time were non-significant for *B. aquilonaris* (Europe: $\rho = 0.58$, $P = 0.108$; Jura: $\rho = -0.23$, $P = 0.552$), for *C. tullia* (Europe: $\rho = 0.17$, $P = 0.678$; Jura: $\rho = -0.12$, $P = 0.764$) and *L. helle* (Europe: $\rho = 0.60$, $P = 0.097$; Jura: $\rho = 0.09$, $P = 0.814$). Although not all significant, we found positive relationships between changes in habitat quality and Ne over time at the European scale (*B. aquilonaris*: $\rho = 0.62$, $P = 0.076$; *C. tullia*: $\rho = 0.63$, $p = 0.068$; *L. helle*: $\rho = 0.71$, $P = 0.033$) but not in the Jura massif (*B. aquilonaris*: $\rho = -0.02$, $P = 0.982$; *C. tullia*: $\rho = -0.04$, $p = 931$; *L. helle*: $\rho = -0.15$, $P = 0.708$). The decrease in mean temperatures and increase in isothermality coincided with a reduction in Ne by 1.6 for the three species (Figures 4 and 6). Climatically suitable areas remained nearly stable (*B. aquilonaris*) or slightly increased (*C. tullia* and *L. helle*) between the end of the Holocene and current days (Figure 6). However, in the same period, Ne changes revealed dramatic population declines for *B. aquilonaris* (decrease factor ~47) and *C. tullia* (decrease factor ~83), and a decline of lower amplitude in *L. helle* (decrease factor ~3).

4. Discussion

4.1 Same past history but different metapopulation functioning

The reconstructions of species demographic history show a common pattern of recent post-glacial population decline and fragmentation among the three species. Despite the ice covered most of their current range during the LGM, and habitat quality and quantity strongly varied at the Europe and Jura scales from the LIG to the Mid-Holocene (~6 kya), the effective population size remained nearly constant or only moderately decreased (by 1.6-fold) over this period (Figure 4). This suggests that the local populations have been able to track their thermal niche over time, probably by moving northward or upslope with glacier retreat (Figure 6; Supplementary Figures S6 to S8). Yet, our assessment of the effect of past climate changes on species demographic history revealed a positive relationship between the changes in habitat quality and the changes in effective population size over time at the European scale, which support a global-scale relationship between climate suitability and population size (Chattopadhyay et al., 2019). After the LGM, glacier retreat opened new habitats in northern Europe while the potential distribution of the three species progressively fragmented into small mountain areas in the South.

The Jura massif corresponds to one of the small areas at the warm range margin (Figures 5 and 6). Contrary to the general warming in many areas of Europe, the temperature continued to decrease in the Jura massif until 14–17 kya (Figure 5 and 6). During the LGM, the northern part of the massif was free of ice, with highly favorable habitats restricted to the margin of the ice sheet (Figure 5; Lhosmot et al., 2022). However, these habitats rapidly became less favorable for the presence of the three species, which might have partly moved their distribution further West. The lack of relationship between climate suitability and population size at the scale of the Jura massif supports the hypothesis that local populations shifted their distribution to track suitable habitats while maintaining nearly constant population size. Since 13–14 kya, the warming created new and more suitable habitats in the Jura massif for *B. aquilonaris* and *L. helle*, whereas habitat quantity and quality remained low elsewhere in Europe (Figure 6).

This result suggests that the Jura massif has provided a climatic refuge for these two species, but not for *C. tullia*, as habitat quality and quantity remained low until 6 kya. The North-to-South gradient of decreasing genetic diversity observed for *B. aquilonaris* and *C. tullia*, together with a more ancient divergence of populations in the northern region of the massif (RUS) common to all species, support a progressive re-colonization of the Jura massif from the northern deglaciated area. This confirms the position of the North of the Jura massif as a glacial refuge for boreo-montane butterflies (Sherpa et al., 2022). Finally, during the Holocene, we found an increase in habitat quality and quantity for all species, probably linked to the formation of peatlands in parallel with the progressive retreat of the Jura glaciers (from 5.8 to 12.9 kya; Gauthier et al., 2019; Lhosmot et al 2022). However, the three species kept declining during this period (Figures 4 and 6), which could reflect the influence of micro-climatic conditions and land uses by humans rather than global climate in recent times (Settele et al., 2008; Noreika et al., 2016).

The spatial distribution of genetic diversity reveals different metapopulation source-sink dynamics between species (Figure 2; Table 1; Supplementary Table S4). Contrary to *B. aquilonaris* and *C. tullia* (diverse pool in the North), the most diverse populations of *L. helle* are currently found in the central region of the massif (DDV; see also Habel et al., 2010), while the relictual northern populations are experiencing genetic erosion. Furthermore, populations of *C. tullia* and *L. helle* in this central region show high genetic connectivity, suggesting that the core of the metapopulation is shifting from RUS to DDV, which is confirmed by genetic differentiation indices (F_{ST}) (Supplementary Table S6 and S8) and field estimates of population density (Duflo et al., 2017). Most populations are not at drift-migration equilibrium (positive population-specific F_{ST} and F_{IS}). As the three species are short dispersers (Baguette, 2003; Gorbach, 2011; Turlure et al., 2014; Wainwright, 2005), small changes in the level of population connectivity can break down the metapopulation functioning, by reducing the

colonization probability of empty patches of habitat, and by increasing the extinction risk in highly isolated patches through genetic drift and inbreeding depression (Hansson, 1991; Hess, 1996; Gaggiotti, 2003; Perry and Lee, 2019).

4.2 Close climatic niches but species-specific requirements

Species climate niche models reveal that the presence of *B. aquilonaris*, *C. tullia* and *L. helle* is determined by the same bioclimatic predictors, which can be explained by their common habitat requirements. These cold-adapted butterflies all live in cold and humid habitats, such as bogs, mires or their margins (Turlure et al., 2010; Habel et al., 2011; Weking et al., 2013). Accordingly, two common predictors of their geographic distribution include a low mean annual temperature (BIO1 < 11°C) and a weak to moderate temperature variability within an average month relative to the year (BIO3). Over their life cycle, the three species need a range of temperatures compatible with (1) the maintenance of soil water saturation for larval development, in relation to the ecology of their host-plants that grow on waterlogged soils (Čelik and Vreš, 2018; Goffart et al., 2014; Price et al., 1998; Schweingruber et al., 2020; Turlure et al., 2010), and (2) imagos thermoregulation activities during the flight period, essential for reproduction success (Kingsolver, 1983; Saastamoinen and Hanski, 2008). They are also equally constrained to areas with even precipitations throughout the year (BIO15), required to maintain the hydrological quality of their habitat (Čelik and Vreš, 2018; Goffart et al., 2014; Turlure et al., 2013).

Each species occupies a slightly distinct climatic niche despite large overlap in temperature (70%) and precipitation seasonality (90%) ranges. For instance, mean temperature of the wettest quarter (BIO8) was the third relevant predictor for the presence of *B. aquilonaris* and *C. tullia*. However, their niche is quite different (only ~40% of overlap) as *B. aquilonaris* tolerates more negative temperatures than *C. tullia* (Table 3), which can be explained by

differences in their biology and ecology. *B. aquilonaris* overwintering 1st instar caterpillars are buffered from negative temperature inside *Sphagnum* hummocks (Turlure et al., 2010; Turlure et al., 2013). In contrast, during flooding events, 3rd instar *C. tullia* caterpillars must actively climb up the stem of the host-plant (Joy and Pullin, 1997; Joy and Pullin, 1999), which requires temperature warm enough. The climatic niche of *C. tullia* also appears to be more constrained than the two other species, as five of the six variables used in SDMs contribute to its predicted distribution by more than 10% (Table 3). The geographic distribution of *C. tullia* excludes elevated areas (> 1,000 masl), where the mean diurnal temperature range is too high (BIO2 > 6°C). By contrast, *L. helle* overwinters as a pupa, with no less than 300 days spent at this stage. Pupal stage microclimatic requirements are not well known (Turlure et al., 2014) but our results suggest that it needs to be shielded from frost (Table 3). Such conditions are found under the vegetation litter where the last stage caterpillar shelters to pupate (Fisher et al., 2014). Out of the three species, *L. helle* is the most thermophilic (BIO1 > 0°C) and the less dependent on soil water saturation as its host-plant, *B. officinalis*, is widely distributed. Our demographic inferences also suggest that this species is the less vulnerable to habitat degradation and climate change, as its population has experienced much more limited decline as compared to the two other species.

The Jura massif constituted a thermal refuge for the three butterfly species during the last glacial cycle and continues in the current context of global warming. The massif included suitable areas for *B. aquilonaris* and *L. helle* over time since the LIG, suggesting they have persisted locally throughout the last glacial cycle (Figure 5). However, for *C. tullia*, local conditions were unfavorable from 17,0 to 4,2 kya (Figure 6). This species is currently found in the massif in fenlands mainly composed of *Carex spp.*, that are more abundant in warmer peatlands than in cold ombotrophic bogs characterized by plant community dominated by *Sphagnum spp*. (Dieleman et al., 2015). The formation of fenlands, which requires sufficiently

high temperature, were probably not encountered locally until the Mid-Holocene in the Jura massif, explaining that local conditions were unfavorable for *C. tullia*. Although the three species probably responded to Pleistocene climatic events by shifting their distribution, the improvement of climate conditions over the past 4,000 years in the Jura massif, and the associated increase in habitat availability, did not slow down the prolonged and ongoing decline of populations. Furthermore, they currently occupy habitats in which temperature conditions correspond to the upper limits of their respective thermal niches. Together, these results suggest that boreo-montane species are somehow trapped in isolated areas (south margin) and in their specific habitat (fragmented patches) (see also Sherpa et al., 2022). This implies that species might not be able to respond to future climate change, especially for dispersal-limited and habitat specialist species (Habel et al., 2023), and that further habitat degradation threaten the persistence of populations.

4.3 Conservation implications

The three species under study are not equally vulnerable to climate change. Based on population genomics analyses and ecological models, *C. tullia* appears to be more affected than *B. aquilonaris* and *L. helle*. Interestingly, their conservation status at the European scale ranks differently, in accordance to their predicted range in Europe: *L. helle* is classified by the IUCN (https://www.iucnredlist.org) as endangered (EN), *C. tullia* as vulnerable (VU) while *B. aquilonaris* is of least concern (LC). As one of the last areas sheltering *B. aquilonaris*, *C. tullia* and *L. helle* in South-Western Europe, the French Jura region is of priority concern. All species are currently experiencing a dramatic decline in this region, which justifies the integration of management measures into the national and regional action plans for their conservation (Houard and Jaulin, 2018; Jacquot et al., 2022).

Species conservation relies on two main axes: the restoration/improvement of habitat buffering against climate change and of landscape connectivity to ensure a dynamic metapopulation functioning (Bennett et al., 2021). In this context, the present multi-taxa study represents a major step towards a better knowledge on the evolutionary history, species-specific ecological requirements, and local dynamics of populations. The genetic erosion and geographic isolation of populations in the Jura massif make them particularly vulnerable to ongoing climate change. For instance, the karstic nature of the massif ground makes it more sensitive to droughts (Bidault et al., 1990). The repetition of dry summers these last years could strongly affect the hydrological equilibrium of the species habitats, and the vegetation structures protecting them from extreme temperatures during summer and winter. In addition to climate conditions, human activities and infrastructures development are other drivers of population trends, as peat cutting, the modification of waterbeds, and the installation of drainage systems to develop agriculture in the massif, which disturb bogs hydrological functioning and peat ecosystems (Gauthier et al., 2019). Indeed, the degradation of wetlands is well documented throughout Europe, due to increased global demand for land and water, pollution, and climate change. Their role as biodiversity hotspots and their contribution for many ecosystem services, such as carbon sequestration and climate change adaptation, stress an urgent need to protect and restore these fragile ecosystems (Kimmel and Mander, 2010; Joosten, 2015; Cartwright, 2019). Measures impeding global warming effects on the hydrological functioning of species habitat are essential, especially with the accumulation of drought events. Concrete solutions include avoidance of additional water withdrawals in peatlands by obliteration of drainage ditches and restoration of historical streambeds.

Our study, combining population genomics analyses and species distribution modeling, confirms the power of these approaches to provide valuable regional-scale recommendations for protecting species (Forester et al., 2013; Supple and Shapiro, 2018). First, genomics (as

opposed to genetics based on a few markers) is particularly precious in conservation biology that focuses on endangered species with low population sizes, because it allows low local sampling size. The low number of individuals collected per locality is compensated by the high number of loci genotyped: instead of averaging heterozygosity across individuals for a few markers to estimate genetic diversity, heterozygosity is averaged across loci, which allows a more precise (lower variance) estimation of local genetic diversity, even when only few individuals are sampled (Nazareno et al., 2017; Després et al., 2019). Contrary to global genetic parameters, the estimation of effective population size requires larger sample sizes, especially for recent demographic events (Robinson et al., 2014; Nunziata and Weisrock, 2018; McLaughlin and Winker, 2020). For this purpose, we considered the species-level (96 gene copies) estimates of site frequency spectrum to infer demographic dynamics, but we also show that robust inference can be obtained with smaller sample sizes (Figure S5). Second, we identify several groups of isolated populations suffering from drift and genetic erosion in the Jura massif, especially in the southernmost region where populations might be more vulnerable to extinction. Because the northernmost region harbors the highest population diversity for two of the studied species, conservation actions may focus on habitat restoration to maintain these diverse gene pools, and on improving landscape connectivity to allow migration to southern recipients. More precise management recommendations may arise from a fine scale study to identify functional ecological corridors (i.e., landscape factors that favor gene flow) and new or former suitable habitat patches for future colonization, which can guide population management (Savary et al., 2021; Osborne et al., 2022), especially improving landscape connectivity to promote the natural movement of species, which can be combined with the reinforcement or reintroduction of populations via assisted migration (Andersen et al., 2014; Descimon and Bachelard, 2014).

5. Conclusions

The use of genomics in conservation is still limited and usually tackles single species, which is only part of larger conservation activities aiming to restore and conserve entire habitats (Sucháckova Bartonová et al., 2023). The analyses of population genomes and species distributions are powerful tools to better understand the genomic and demographic consequences of climate changes over time and to inform conservation decisions. By integrating the output of both approaches, our study sheds light not only on the current population dynamics, but also on the species abilities to respond to past climate changes, and therefore on their vulnerability to ongoing climate change. Furthermore, we determine that multiple co-distributed species have a shared demographic and biogeographic history, due to similar habitat and climate niche, and recolonization history. Such knowledge is essential to better predict community-scale responses to climate warming, and to implement conservation actions that can benefit multiple species. Nonetheless, we also found idiosyncratic responses to habitat fragmentation at the local scale, which might be explained by specific species traits and distinct metapopulation dynamics. This allows identifying the species that might be more vulnerable to extinction and areas that might act as diversity reservoirs. Incorporating our comparative approach with time series genomic data (Díez-del-Molino et al., 2018; Clark et al., 2023) can further help evaluating the effect of management practices on population connectivity and effective size over time, and/or identify source/sink populations for future reintroduction or reinforcement actions.

Supplementary material

Additional supporting information may be found in the online version of the article at the publisher's website.

Data accessibility

The ddRAD sequences (fastq) are available at the European Nucleotide Archive repository (http://www.ebi.ac.uk/ena) and accessible under study accession numbers PRJEB65448. The SNP datasets are available at Dryad Digital Repository (DOI: 10.5061/dryad.pk0p2ngt1). In accordance with the French regulation regarding protected species (article L.124-4 of the environment code), the precision of coordinates of the localities sampled in the Jura massif was degraded to 10 × 10 km uncertainty but are available from authors upon request. The GBIF occurrence datasets are available at https://doi.org/10.15468/dl.3gc8xu (*C. tullia*), https://doi.org/10.15468/dl.cjnunz (*B. aquilonaris*) and https://doi.org/10.15468/dl.tbwmfm (*L. helle*).

Declaration of competing interest

There is no conflict of interest.

References

Alexander, D. H., Novembre, J., & Lange, K. (2009). Fast model-based estimation of ancestry in unrelated individuals. *Genome Research*, *19*, 1655–1664. https://doi.org/10.1101/gr.094052.109%20

Andersen, A., Simcox, D. J., Thomas, J. A., & Nash, D. R. (2014). Assessing reintroduction schemes by comparing genetic diversity of reintroduced and source populations: A case study of the globally threatened large blue butterfly (Maculinea arion). *Biological Conservation*, *175*, 34–41. https://doi.org/10.1016/j.biocon.2014.04.009

Araùjo, M. B., & New, M. (2007). Ensemble forecasting of species distributions. *Trends in Ecology and Evolution*, *22*(1), 42–47. https://doi.org/10.1016/j.tree.2006.09.010

Baguette, M. (2003). Long distance dispersal and landscape occupancy in a metapopulation of the cranberry fritillary butterfly. *Ecography*, *26*, 153–160.

Bauerfeind, S. S., Theisen, A., & Fischer, K. (2009). Patch occupancy in the endangered butterfly *Lycaena helle* in a fragmented landscape: effects of habitat quality, patch size and isolation. *Journal of Insect Conservation*, *13*, 271–277. https://doi.org/10.1007/s10841-008-9166-1

Bennett, J. M., Sunday, J., Calosi, P., Villalobos, F., Martinez, B., Molina-Venegas, R., Araùjo, M. B., Algar, A. C., Clusella-Trullas, S., Hawkins, B. A., Keith, S. A., Kühn, I., Rahbek, C., Rodriguez, L., Singer, A., Morales-Castilla, I., & Olalla-Tárraga, M.-A. (2021). The evolution of critical thermal limits of life on Earth. *Nature Communications*, *12*, 1198. https://doi.org/10.1038/s41467-021-21263-8

Bidault, M., Rosenthal, P., Magny, M., Richard, H., Perrier, P., Cretin, Y., Robert, J.-C., Prouteau, C., Robert, J.-Y., Craney, E., Michelat, D., Mangin, M., Petitjean, M., Laurent, H., Raissouni, B., Gresser, P., Gresset, M., Mayaud, J.-L., Charles-Lyet, G., … Royer, C. (1990). *Le Parc Naturel du Haut-Jura: son milieu naturel, son histoire et ses activités*. (290 p. ; Centre Universitaire d'Etudes Régionales). Université de Franche-Comté.

Brown, J. L., Hill, D. J., Dolan, A. M., Carnaval, A. C., & Haywood, A. M. (2018). PaleoClim, high spatial resolution paleoclimate surfaces for global land areas. *Nature*, *5*(180254). https://doi.org/10.1038/sdata.2018.254

Bushnell, B. (2014). *BBMap: A Fast, Accurate, Splice-Aware Aligner*. United States: N. p.

Cartwright, J. (2019). Ecological islands: conserving biodiversity hotspots in a changing climate. *Frontiers in Ecology and the Environment, 17(6)*, 331-340. https://doi.org/10.1002/fee.2058

Čelik, T., & Vreš, B. (2018). Microtopography determines the habitat quality of a threatened peatland butterfly at its southern range margin. *Journal of Insect Conservation*, *22*, 707–720. https://doi.org/10.1007/s10841-018-0095-3

Chattopadhyay, B., Garg, K. M., Ray, R., & Rheindt, F. E. (2019). Fluctuating fortunes: genomes and habitat reconstructions reveal global climate-mediated changes in bats' genetic diversity. *Proceedings of the Royal Society B*, *289*(1944), 20190304. https://doi.org/10.1098/rspb.2019.0304

Chuluunbaatar, G., Barua, K. K., & Muehlenberg, M. (2009). Habitat association and movement patterns of the violet copper (*Lycaena helle*) in the natural landscape of West Khentey in Northern Mongolia. *Journal of Entomology and Nematology*, *1*(5), 56–63. https://academicjournals.org/JEN

Clarke, H. E. (2022). A provisional checklist of European butterfly larval foodplants. *Nota Lepidopterologica*, *45*, 139–167. https://doi.org/10.3897/nl.45.72017

Clark, R. D., Catalano, K. A., Fitz, K. S., Garcia, E., Jaynes, K. E., Reid, B. N., ... & Pinsky, M. L. (2023). The practice and promise of temporal genomics for measuring evolutionary responses to global change. *Molecular Ecology Resources*. https://doi.org/10.1111/1755-0998.13789

Cornuet, J.-M., Pudlo, P., Veyssier, J., Dehne-Garcia, A., Gautier, M., Leblois, R., Marin, J.-M., & Estoup, A. (2014). DIYABC v2.0: a software to make approximate Bayesian computation inferences about population history using single nucleotide polymorphism, DNA sequence and microsatellite data. *Bioinformatics*, *30*(8), 1187–1189. https://doi.org/10.1093/bioinformatics/btt763

Danecek, P., Auton, A., Abecasis, G., Albers, C. A., Banks, E., DePristo, M. A., Handsaker, R. E., Lunter, G., Marth, G. T., Sherry, S. T., McVean, G., Durbin, R., & 1000 Genomes Project

Analysis Group. (2011). The variant call format and VCFtools. *Bioinformatics*, *27*(15), 2156–2158.

Decoin, R., Mazuez, C., Gens, H., Gagnaison, C., Genin, C., Tissot, B., & Cochard, A. (2022). *Etude sur le Fadet des tourbières (Coenonympha tullia) sur les populations du vallon de la Bonavette ; Démographie, écologie, répartition spatiale, capacité de déplacement et dispersion*. (63 p. + annexes). Les amis de la réserve naturelle du lac de Remoray. 10.13140/RG.2.2.35935.33447

Dennis, R. L. H., & Eales, H. T. (1997). Patch occupancy in *Coenonympha tullia* (Müller, 1764) (Lepidoptera: Satyrinae): habitat quality matters as much as patch size and isolation. *Journal of Insect Conservation*, *1*, 167–176.

Descimon, H., & Bachelard, P. (2014). Results of two introductions of Lycaena helle in France. In *Jewels in the Mist: A synopsis on the highly endangered butterfly species the Violet Copper, Lycaena helle*. (Eds Habel, J. C., Meyer, M, Schmitt, T, 246 p.). Pensoft ISBN 978-954-642-721-2.

Devictor, V., van Swaay, C., Brereton, T., Brotons, L., Chamberlain, D., Heliölä, J., Herrando, S., Julliard, R., Kuussaari, M., Lindström, Å., Reif, J., Roy, D. B., Schweiger, O., Settele, J., Stefanescu, C., Van Strien, A., Van Turnhout, C., Vermouzek, Z., Wallis De Vries, M., … Jiguet, F. (2012). Differences in the climatic debts of birds and butterflies at a continental scale. *Nature Climate Change*, *2*, 121–124. https://doi.org/10.1038/nclimate1347

Dieleman, C. M., Branfireun, B. A., McLaughlin, J. W., & Lindo, Z. (2015). Climate change drives a shift in peatland ecosystem plant community: Implications for ecosystem function and stability. *Global Change Biology*, *21*, 388–395. https://doi.org/doi: 10.1111/gcb.12643

Díez-del-Molino, D., Sánchez-Barreiro, F., Barnes, I., Gilbert, M. T. P., & Dalén, L. (2018). Quantifying temporal genomic erosion in endangered species. *Trends in Ecology & Evolution*, *33*(3), 176-185. https://doi.org/10.1016/j.tree.2017.12.002

Duflo, C., Jacquot, P., Mora, F., & Ryelandt, J. (2017). *Plan régional d'action en faveur des rhopalocères*. (83 p. + annexes). Conservatoire botanique national de Franche-Comté – Observatoire régional des Invertébrés. https://cbnfc-ori.org/espace-documentation/plan-regional-d-action-en-faveur-des-rhopaloceres-2017

Estrada, A., Morales-Castilla, I., Meireles, C., Caplat, P., & Early, R. (2017). Equipped to cope with climate change: traits associated with range filling across European taxa. *Ecography*, *41*(5), 770–781. https://doi.org/10.1111/ecog.02968

Fick, S. E., & Hijmans, R. J. (2017). WorldClim 2: new 1-km spatial resolution climate surfaces for global land areas. *International Journal of Climatology*, *37*, 4302–4315. https://doi.org/10.1002/joc.5086

Fischer, K., Beinlich, B., & Plachter, H. (1999). Population structure, mobility and habitat preferences of the violet copper *Lycaena helle* (Lepidoptera: Lycaenidae) in Western Germany: implications for conservation. *Journal of Insect Conservation*, *3*, 43–52.

Fisher, K., Schubert, E. & Limberg, J. (2014). Caught in a trap: How to preserve a post-glacial relict species in secondary habitat? In *Jewels in the Mist: A synopsis on the highly endangered butterfly species the Violet Copper, Lycaena helle*. (Habel J. C., Meyer, M, Schmitt, T ,246 p.). Pensoft.

Forester, B. R., DeChaine, E. G., & Bunn, A. G. (2013). Integrating ensemble species distribution modelling and statistical phylogeography to inform projections of climate change impacts on species distributions. *Diversity and Distributions*, *19*(12), 1480-1495. https://doi.org/10.1111/ddi.12098

Fourcade, Y., Engler, J. O., Rödder, D., & Secondi, J. (2014). Mapping Species Distributions with MAXENT Using a Geographically Biased Sample of Presence Data: A Performance Assessment of Methods for Correcting Sampling Bias. *PLoS ONE*, *9*(5). https://doi.org/10.1371/journal.pone.0097122

Frichot, E., & François, O. (2015). LEA: An R package for landscape and ecological association studies. *Methods in Ecology and Evolution*, *6*, 925–929. https://doi.org/10.1111/2041-210X.12382

Gaggiotti, O. E. (2003). Genetic threats to population persistence. *Annales Zoologici Fennici*, *40*, 155–168.

Gauthier, E., Jassey, V. E. J., Mitchell, E. A. D., Lamentowicz, M., Payne, R., Delarue, F., Laggoun-Defarge, F., Gilbert, D., & Richard, H. (2019). From Climatic to Anthropogenic Drivers: A Multi-Proxy Reconstruction of Vegetation and Peatland Development in the French Jura Mountains. *Quaternary*, *2*(4), 38. https://doi.org/10.3390/quat2040038

GBIF.org. (2022). *GBIF Occurrence download Coenonympha tullia (Müller, 1764), Boloria aquilonaris (Stichel, 1908), Lycaena helle (Denis & Schiffermüller, 1775).* https://doi.org/10.15468/dl.3gc8xu; https://doi.org/10.15468/dl.cjnunz; https://doi.org/10.15468/dl.tbwmfm

Gorbach, V. V. (2011). Spatial Distribution and Mobility of Butterflies in a Population of the Cranberry Fritillary *Boloria aquilonaris* (Lepidoptera, Nymphalidae). *Russian Journal of Ecology*, *42*(4), 321–327. https://doi.org/10.1134/S1067413611040060

Goffart, P., Cavelier, E., Lighezzolo, P., Rauw, A., & Lafontaine, D. (2014). Restoration and management of habitat networks for Lycaena helle in Belgium. In *Jewels in the Mist: A synopsis on the highly endangered butterfly species the Violet Copper, Lycaena helle*. (Habel J. C., Meyer, M, Schmitt, T ,246 p.). Pensoft.

Goudet, J. (2005). HIERFSTAT, a package for R to compute and test hierarchical F-statistics. *Molecular Ecology Notes*, *5*, 184–186. https://doi.org/10.1111/j.1471-8278 .2004.00828.x

Habel, J. C., Finger, A., Schmitt, T., & Nève, G. (2011). Survival of the endangered butterfly *Lycaena helle* in a fragmented environment: Genetic analyses over 15 years. *Journal of Zoological Systematics and Evolutionary Research*, *49*(1), 25–31. https://doi.org/10.1111/j.1439-0469.2010.00575.x

Habel, J. C., Werner, U., Gros, P., Teucher, M. & Schmitt T. (2023). Butterfly species respond differently to climate warming and land use change in the northern Alps. *Science of the Total Environment*, 890. https://doi.org/10.1016/j.scitotenv.2023.164268

Hansson, L. (1991). Dispersal and connectivity in metapopulations. *Biological Journal of the Linnean Society*, *42*, 89–103.

Heikkinen, R. K., Luoto, M., Leikola, N., Pöyry, J., Settele, J., Kudrna, O., Marmion, M., Fronzek, S., & Thuiller, W. (2010). Assessing the vulnerability of European butterflies to climate change using multiple criteria. *Biodiversity Conservation*, *19*, 695–723. https://doi.org/10.1007/s10531-009-9728-x

Hess, G. R. (1996). Linking Extinction to Connectivity and Habitat Destruction in Metapopulation Models. *The American Naturalist*, *148*(1), 226–236. https://doi.org/10.1086/285922

Hewitt, G. (2000). The genetic legacy of the Quaternary ice ages. *Nature*, *405*, 907–913.

Hewitt, G. M. (2004). Genetic consequences of climatic oscillations in the Quaternary. *Philosophical Transactions of the Royal Society B*, *359*, 183–195. https://doi.org/10.1098/rstb.2003.1388

Houard, X., & Jaulin, S. (2018). *Plan national d'actions 2018-2028 En faveur des papillons de jour* (64 p.). French Ministry of Ecological and Solidary Transition. https://papillons.pnaopie.fr/wp-content/uploads/2020/04/PNA-Papillons-de-jour-France-metropolitaine-2018-2028.pdf

Jacquot, P., Itrac-Bruneau, R., Barbotte, Q., Mora, F., & Ryelandt, J. (2022). *Déclinaison régionale du Plan National d'Actions en faveur des papillons de jour - Bourgogne-Franche-Comté 2021-2030. Agir pour la préservation de nos papillons de jour et zygènes parimoniaux*. (231 p.). Conservatoire Botanique National de Franche-Comté - Observatoire régional des Invertébrés. https://cbnfc-ori.org/insectes-invertebres/espece-vegetale/declinaison-regionale-du-plan-national-dactions-en-faveur-des?utm_campaign=Publications%20techniques%20Entomo&utm_medium=email&utm_source=Mailjet

Joosten, H. (2015). *Peatlands, climate change mitigation and biodiversity conservation*. Norden. (15 p.). http://dx.doi.org/10.6207/ANP2015-727

Joy, J., & Pullin, S. (1997). The effects of flooding on the survival and behaviour of overwintering Large heath butterfly *Coenonympha tullia* larvae. *Biological Conservation*, *82*, 61–66.

Joy, J., & Pullin, S. (1999). Field studies on flooding and survival of overwintering Large heath butterfly *Coenonympha tullia* larvae on Fenn's and Whixall Mossess in Shropshire and Wrexham, U.K. *Ecological Entomology*, *24*, 426–431.

Karger, D. N., Nobis, M. P., Normand, S., Graham, C. H., & Zimmermann, N. E. (2020). CHELSA-TraCE21k v1.0. Downscaled transient temperature and precipitation data since the last glacial maximum. *EnviDat*. https://doi.org/10.5194/cp-2021-30

Kebaili, C., Sherpa, S., Rioux, D., & Després, L. (2022). Demographic inferences and climatic niche modelling shed light on the evolutionary history of the emblematic cold-adapted Apollo butterfly at regional scale. *Molecular Ecology*, *31*, 448–466. https://doi.org/10.1111/mec.16244

Keightley, P. D., Pinharanda, A., Ness, R. W., Simpson, F., Dasmahapatra, K. K., Mallet, J., Davey, J. W., & Jiggins, C. D. (2015). Estimation of the Spontaneous Mutation Rate in *Heliconius melpomene*. *Molecular Biology and Evolution*, *32*(1), 239–243. https://doi.org/10.1093/molbev/msu302

Kimmel, K., & Mander, Ü. (2010). Ecosystem services of peatlands: Implications for restoration. *Progress in Physical Geography: Earth and Environment*, *34(4)*, 491–514. https://doi.org/10.1177/0309133310365595

Kingsolver, J. G. (1983). Ecological Significance of Flight Activity in Colias Butterflies: Implications for Reproductive Strategy and Population Structure. *Ecology*, *64*(3), 546–551.

Koscinski, D., Crawford, L. A., Keller, H. A., & Keyghobadi, N. (2011). Effects of different methods of non-lethal tissue sampling on butterflies. *Ecological Entomology*, *36*, 301–308.

Lebigre, C., Turlure, C., Vandewalle, H., Binard, F., Habel, J. C., & Schtickzelle, N. (2022). Diverging effects of geographic distance and local habitat quality on the genetic characteristics of three butterfly species. *Ecological Entomology*, 1–13. https://doi.org/DOI: 10.1111/een.13174

Lhosmot, A., Bouchez, J., Steinmann, M., Lavastre, V., Bichet, V., Loup, C., Stefani, V., Boetsch, A., Chevet, J., Toussaint, M.-L., Gaillardet, J., & Bertrand, G. (2022). The origin and transfer of water and solutes in peatlands: A multi tracer assessment in the carbonated Jura Mountains. *Hydrological Processes*, *36*(12), e14781. https://doi.org/10.1002/hyp.14781

Liu, X., & Fu, Y. X. (2020). Stairway Plot 2: demographic history inference with folded SNP frequency spectra. *Genome Biology*, *21*(280). https://doi.org/10.1186/s13059-020-02196-9

Marmion, M., Parviainen, M., Luoto, M., Heikkinen, R. K., & Thuiller, W. (2009). Evaluation of consensus methods in predictive species distribution modelling. *Diversity and Distributions*, *15*, 59–69. https://doi.org/10.1111/j.1472-4642.2008.00491.x

McLaughlin, J. F., & Winker, K. (2020). An empirical examination of sample size effects on population demographic estimates in birds using single nucleotide polymorphism (SNP) data. *PeerJ*, *8*, e9939. https://doi.org/10.7717/peerj.9939

Nazareno, A. G., Bemmels, J. B., Dick, C. W., & Lohmann, L. G. (2017). Minimum sample sizes for population genomics: an empirical study from an Amazonian plant species. *Molecular Ecology Resources*, *17*(6), 1136-1147. https://doi.org/10.1111/1755-0998.12654

Noreika, N., Kotze, D. J., Loukola, O. J., Sormunen, N., Vuori, A., Päivinen, J., Penttinen, J., Punttila, P., & Kotiaho, J. S. (2016). Specialist butterflies benefit most from the ecological restoration of mires. *Biological Conservation*, *196*, 103–114. https://doi.org/10.1016/j.biocon.2016.02.014

Nunziata, S. O., & Weisrock, D. W. (2018). Estimation of contemporary effective population size and population declines using RAD sequence data. *Heredity*, *120*(3), 196-207. https://doi.org/10.1038/s41437-017-0037-y

O'Leary, S. J., Puritz, J. B., Willis, S. C., Hollenbeck, C. M., & Portnoy, D. S. (2018). These aren't the loci you're looking for: Principles of effective SNP filtering for molecular ecologists. *Molecular Ecology*, *27*, 3193–3206. https://doi.org/10.1111/mec.14792

Osborne, A., & Coulthard, E. (2022). Early dispersion and colony formation of the Large heath butterfly *Coenonympha tullia ssp. davus* following a species reintroduction onto chat moss, Manchester, UK. *British Journal of Entomology and Natural History*, *35*, 81–90.

Parmesan, C., Ryrholm, N., Stefanescu, C., Hill, J. K., Thomas, C. D., Descimon, H., Huntley, B., Kaila, L., Kullberg, J., Tammaru, T., Tennent, W. J., Thomas, J. A., & Warren, M. (1999). Poleward shifts in geographical ranges of butterfly species associated with regional warming. *Nature*, *399*, 579–583.

Pedreschi, D., García-Rodríguez, O., Yannic, G., Cantarello, E., Diaz, A., Golicher, D., Korstjens, A. H., Heckel, G., Searle, J. B., Gillingham, P., Hardouin, E. A., & Stewart, J. R. (2019). Challenging the European southern refugium hypothesis: Species- specific structures versus general patterns of genetic diversity and differentiation among small mammals. *Global Ecology and Biogeography*, *28*, 262–274. https://doi.org/10.1111/geb.12828

Perry, G. L. W., & Lee, F. (2019). How does temporal variation in habitat connectivity influence metapopulation dynamics? *Oikos*, *128*, 1277–1286. https://doi.org/10.1111/oik.06052

Petkova, D., Novembre, J., & Stephens, M. (2015). Visualizing spatial population structure with estimated effective migration surfaces. *Nature Genetics*, *48*, 94–100.

Price, J., Rochefort, L., & Quinty, F. (1998). Energy and moisture considerations on cutover peatlands: surface microtopography, mulch cover and Sphagnum regeneration. *Ecological Engineering*, *10*, 293–312.

QGIS Development Team. (2022). *QGIS Geographic Information System*. (Version 3.22.3) [Computer software]. Open Source Geospatial Foundation Project. http://qgis.osgeo.org

R Core Team. (2022). *R: A language and environment for statistical computing*. R Foundation for Statistical Computing. https://www.R-project.org/

Robinson, J. D., Coffman, A. J., Hickerson, M. J., & Gutenkunst, R. N. (2014). Sampling strategies for frequency spectrum-based population genomic inference. *BMC Evolutionary Biology*, *14*(1), 1-16. https://doi.org/10.1186/s12862-014-0254-4

Rochette, N. C., Rivera- Colón, A. G., & Catchen, J. M. (2019). Stacks 2: Analytical methods for paired- end sequencing improve RADseq- based population genomics. *Molecular Ecology*, *28*, 4737–4754. https://doi.org/10.1111/mec.15253

Saastamoinen, M., & Hanski, I. (2008). Genotypic and Environmental Effects on Flight Activity and Oviposition in the Glanville Fritillary Butterfly. *The American Naturalist*, *171*(6), 701–858. https://doi.org/10.1086/587531

Savary, P., Foltête, J.-C., Moal, H., Vuidel, G., & Garnier, S. (2021). Analysing landscape effects on dispersal networks and gene flow with genetic graphs. *Molecular Ecology Resources*, *21*(4), 1167–1185. https://doi.org/10.1111/1755-0998.13333

Schmitt, T. (2007). Molecular biogeography of Europe: Pleistocene cycles and postglacial trends. *Frontiers in Zoology*, *4*(11). https://doi.org/10.1186/1742-9994-4-11

Schmitt, T., & Varga, Z. (2012). Extra-Mediterranean refugia: The rule and not the exception? *Frontiers in Zoology*, *9*(22). https://doi.org/10.1186/1742-9994-9-22

Schoville, S. D., Stuckey, M., & Roderick, G. K. (2011). Pleistocene origin and population history of a neo-endemic alpine butterfly. *Molecular Ecology*, *20*, 1233–1247. https://doi.org/10.1111/j.1365-294X.2011.05003.x

Schweingruber, F. H., Kučerová, A., Adamec, L., & Doležal, J. (2020). *Anatomic Atlas of Aquatic and Wetland Plant Stems: Vol. Polygonaceae* (Springer, Cham).

Settele, J., Kudrna, O., Harpke, A., Kühn, I., van Swaay, C., Verovnik, R., Warren, M., Wiemers, M., Hanspach, J., Hickler, T., Kühn, E., van Halder, I., Veling, K., Vliegenthart, A., Wynhoff, I., & Schweiger, O. (2008). *Climatic risk atlas of European butterflies* (Pensoft).

Sherpa, S., Kebaili, C., Rioux, D., Guéguen, M., Renaud, J., & Després, L. (2022). Population decline at distribution margins: Assessing extinction risk in the last glacial relictual but still functional metapopulation of a European butterfly. *Diversity and Distributions*, *28*(2), 271–290. https://doi.org/10.1111/ddi.13460

Sucháckova Bartonová, A., Linke, D., Klecková, I., Ribeiro, P. G., & Mastos-Maraví, P. de G. (1-14). Incorporating genomics into insect conservation: Butterflies as a model group. *Insect Conservation and Diversity*. https://doi.org/10.1111/icad.12643

Supple, M. A., & Shapiro, B. (2018). Conservation of biodiversity in the genomics era. *Genome Biology*, *19*, 1-12. https://doi.org/10.1186/s13059-018-1520-3

Taberlet, P., Fumagalli, L., Wust-Saucy, A.-G., & Cosson, J.-F. (1998). Comparative phylogeography and postglacial colonization routes in Europe. *Molecular Ecology*, *7*, 453–464. https://doi.org/10.1046/j.1365-294x.1998.00289.x

Thuiller, W., Georges, D., Guéguen, M., Engler, R., Breiner, F., Lafourcade, B., & Patin, R. (2023). *Package Biomod2. Ensemble Platform for Species Distribution Modeling*. (Version 4.2-2) [R].

Thuiller, W., Lafourcade, B., Engler, R., & Araùjo, M. B. (2009). BIOMOD: a platform for ensemble forecasting of species distributions. *Ecography*, *32*, 369–373. https://doi.org/10.1111/j.1600-0587.2008.05742.x

Turlure, C., Choutt, J., Baguette, M., & Van Dyck, H. (2010). Microclimatic buffering and resource-based habitat in a glacial relict butterfly: significance for conservation under climate change. *Global Change Biology*, *16*, 1883–1893. https://doi.org/10.1111/j.1365-2486.2009.02133.x

Turlure, C., Radchuk, V., Baguette, M., Meijrink, M., van den Burg, A., Wallis De Vries, M., & van Duinen, G.-J. (2013). Plant quality and local adaptation undermine relocation in a bog specialist butterfly. *Ecology and Evolution*, *3*(2), 244–254. https://doi.org/10.1002/ece3.427

Turlure, C., Van Dyck, H., Goffart, P., & Schtickzelle, N. (2014). Resource-based habitat use in Lycaena helle: Significance of a functional, ecological niche-oriented approach. In *Jewels in the Mist: A synopsis on the highly endangered butterfly species the Violet Copper, Lycaena helle*. (Habel J. C. et al., pp. 67–85). Pensoft.

van Swaay, C., Maes, D., Collins, S., Munguira, M. L., Šašic, M., Settele, J., Verovnik, R., Warren, M., Wiemers, M., Wynhoff, I., & Cuttelod, A. (2011). Applying IUCN criteria to invertebrates: How red is the Red List of European butterflies? *Biological Conservation*, *144*, 470–478. https://doi.org/10.1016/j.biocon.2010.09.034

Wainwright, D. (2004). *Conservation and habitat requirements of the large heath butterfly (Coenonympha tullia)*. University of Sunderland. https://ethos.bl.uk/OrderDetails.do?uin=uk.bl.ethos.418240

Warren, M. S., Hill, J. K., Thomas, J. A., Asher, J., Fox, R., Huntley, B., Roy, D. B., Telfer, M. G., Jeffcoate, S., Harding, P., Willis, S. G., Greatorex-Davies, J. N., Moss, D., & Thomas, C. D. (2001). Rapid responses of British butterflies to opposing forces of climate and habitat change. *Nature*, *141*, 65–69. https://doi.org/10.1038/35102054

Weking, S., Hermann, G., & Fartmann, T. (2013). Effects of mire type, land use and climate on a strongly declining wetland butterfly. *Journal of Insect Conservation*, *17*, 1081–1091. https://doi.org/10.1007/s10841-013-9585-5

Figures and figure captions

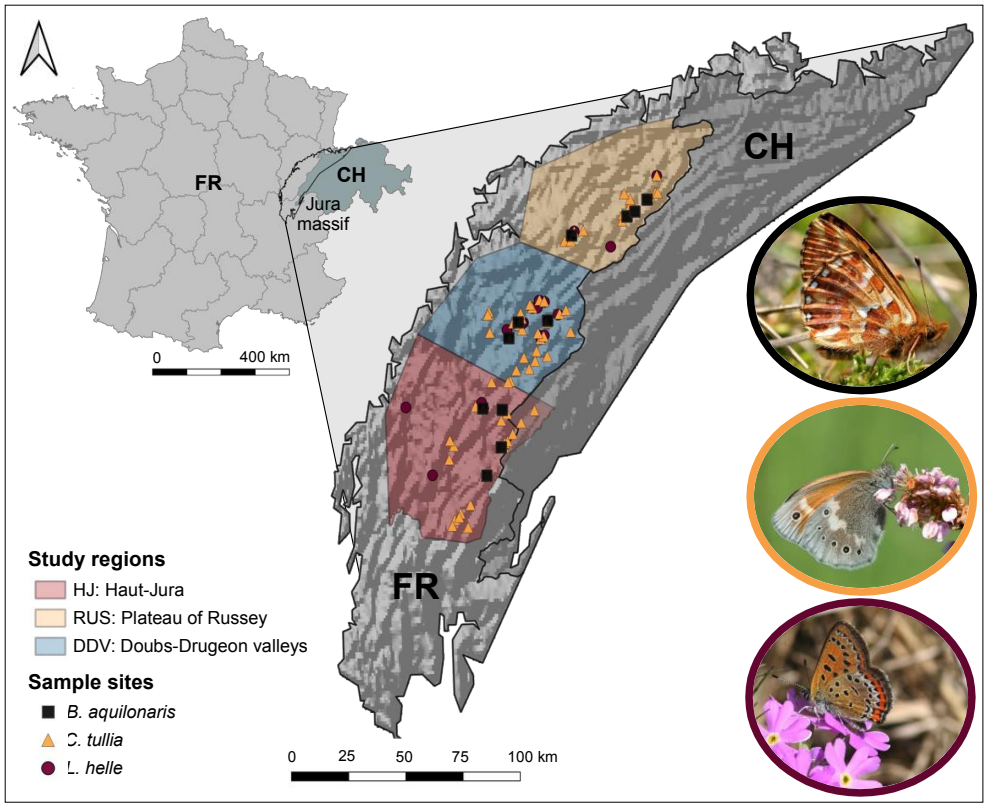

Figure 1. Study area and location of sample sites for the three species. The top left map shows the context of the study area, locating the Jura massif on the border between France (FR) and Switzerland (CH). The enlarged map shows the Jura massif with the three main study regions (HJ; RUS; DDV) in different transparent fill colors. Symbol shape and colors represent the location of sample sites for each species. Photos credits: *B. aquilonaris*, Frédéric Mora; *C. tullia*, Mathilde Poussin; *L. helle*, Pierre Durlet.

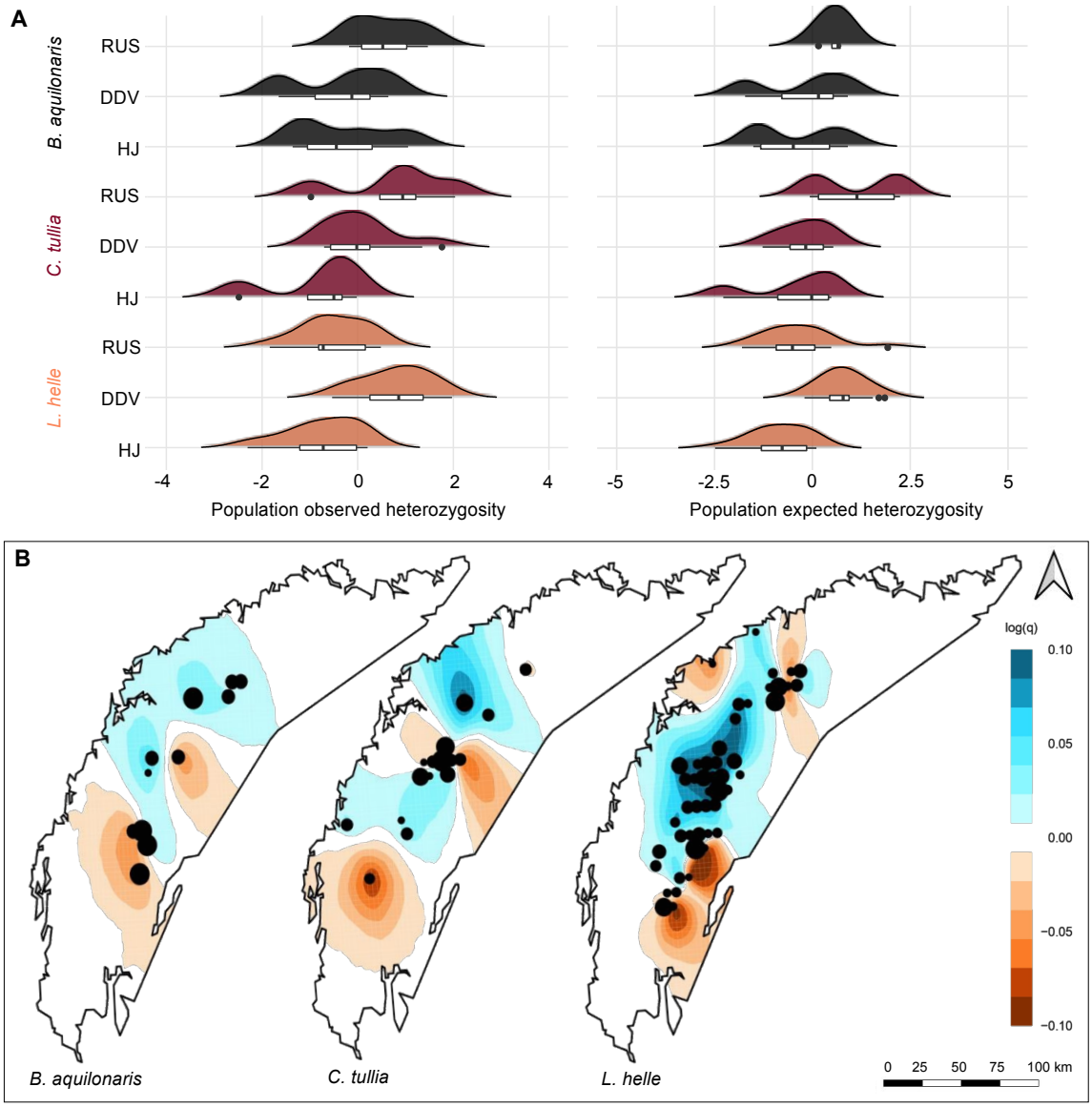

953 **Figure 2. Spatial patterns in genetic diversity.** A) Density and distribution of observed (Ho)
954 and expected (He) heterozygosity (scaled and centered separately for each species) among the
955 three regions, from North (RUS) to South (HJ). B) EEMS contour plots of the average posterior
956 distribution of diversity rates q (log10 scale). Darker font colors show significantly high (blue)
957 or low (brown) within-deme genetic dissimilarities.

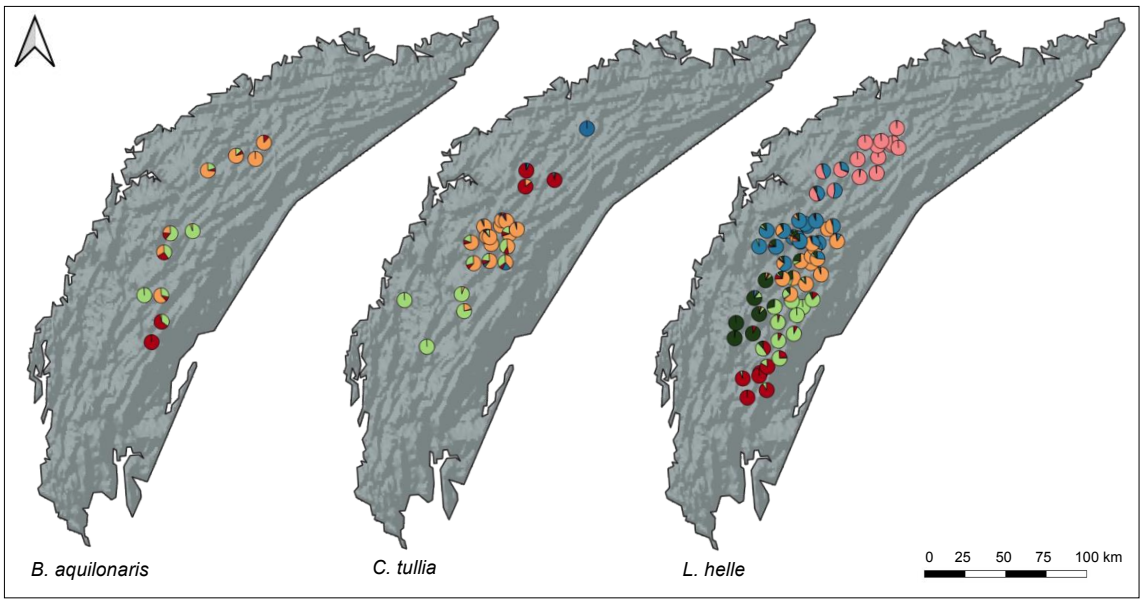

Figure 3. Genetic differentiation among regions. Average ancestry coefficients among individuals per sampling locality, estimated from ADMIXTURE analyses for A) *B. aquilonaris* (K = 3) B) *C. tullia* (K=4) and C) *L. helle* (K=6).

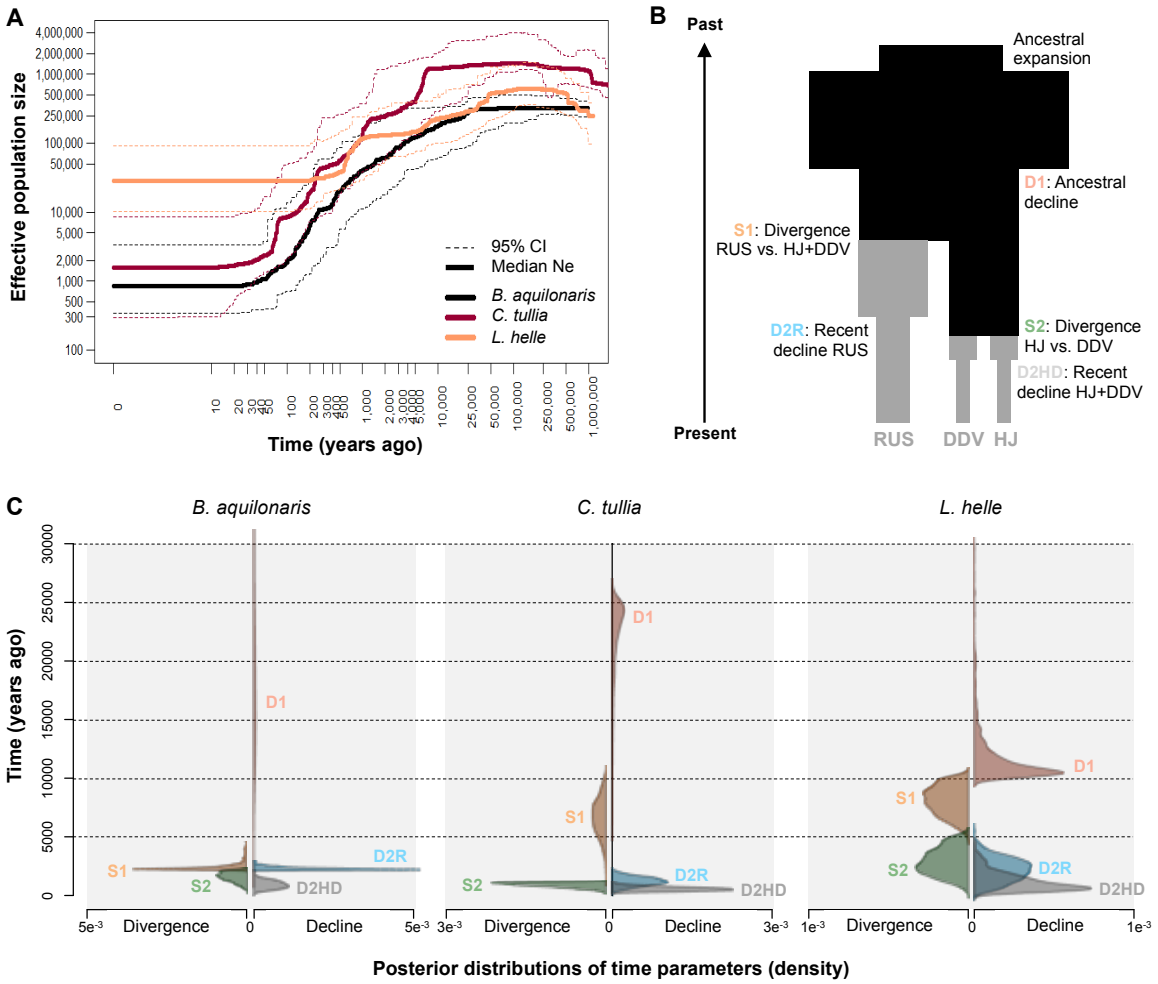

Figure 4. Population demographic history. A) Changes in effective population size (Ne) over time based on the species-level SFS (all regions combined) using Stairway Plot v2. Full-colored lines: median Ne; dotted lines: 95% confidence intervals (CI) generated from 200 bootstrap replicates (population-level analyses in Supplementary Figure S5). B) Schematic representation of the best divergence scenario for the three species using DIYABC (see Table 2 for identification of best scenario). C) Estimated divergence and decline times for the best scenario presented in B (posterior distributions for the 1% simulated data closest to the observed data).

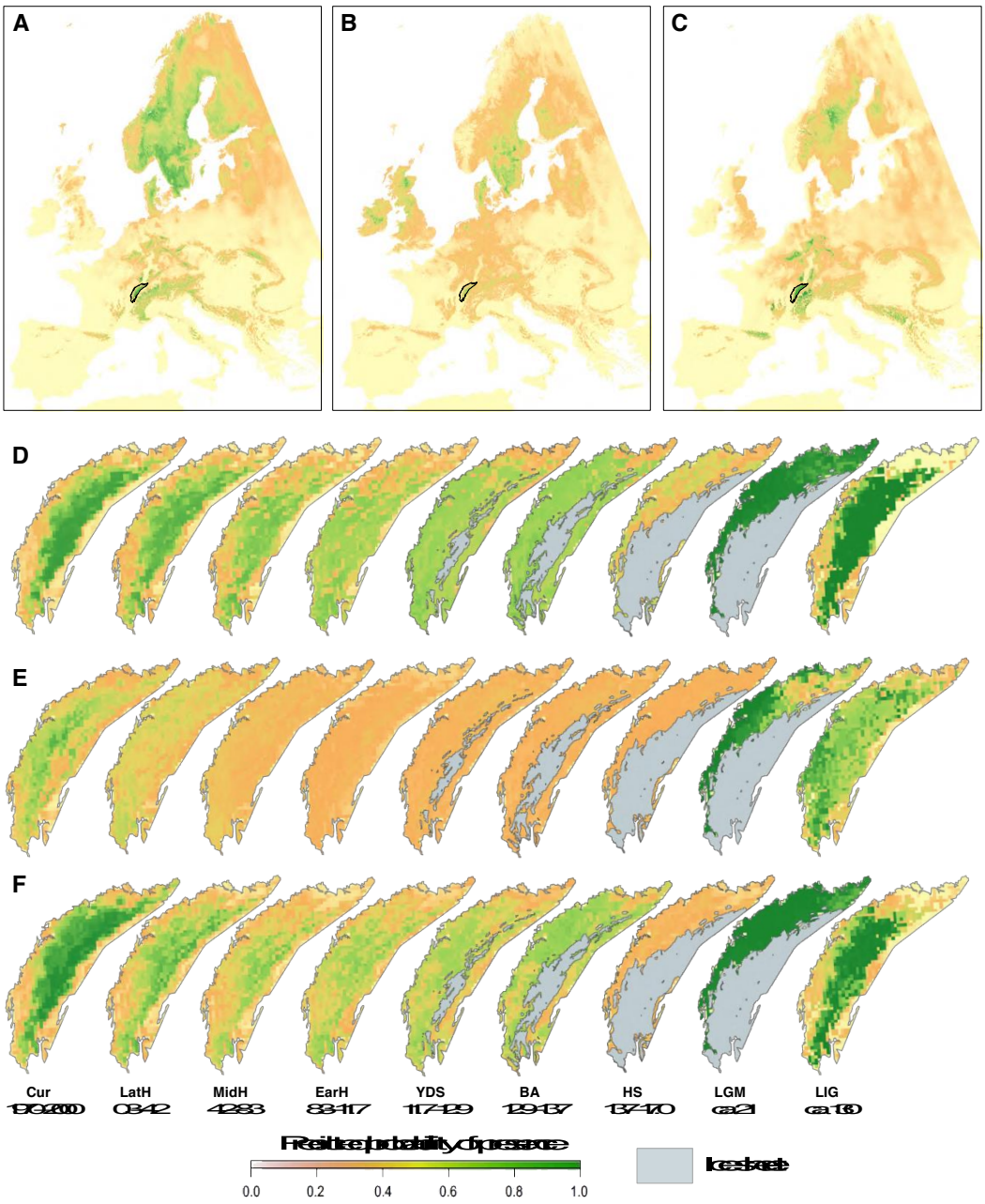

Figure 5. Changes in species potential distribution over time in the Jura massif. Species potential distribution at the European scale based on six bioclim variables (BIO1, BIO2, BIO3, BIO8, BIO12, BIO15) under current conditions for A) *B. aquilonaris* B) *C. tullia* and C) *L. helle*. Predicted distributions under current climate (Cur) and palaeoclimates in the Jura massif (predicted distributions at the European scale are in Supplementary Figures S6 to S8) for D) *B. aquilonaris* E) *C. tullia* and F) *L. helle*. Paleoclimates (in kya): Late Holocene (LatH); Mid Holoecen (MidH); Early Holocene (EarH); Younger Dryas Stadial (YDS); Bølling-Allerød (BA); Heinrich Stadial 1 (HS); Last Glacial Maximum (LGM); Last Interglacial (LIG).

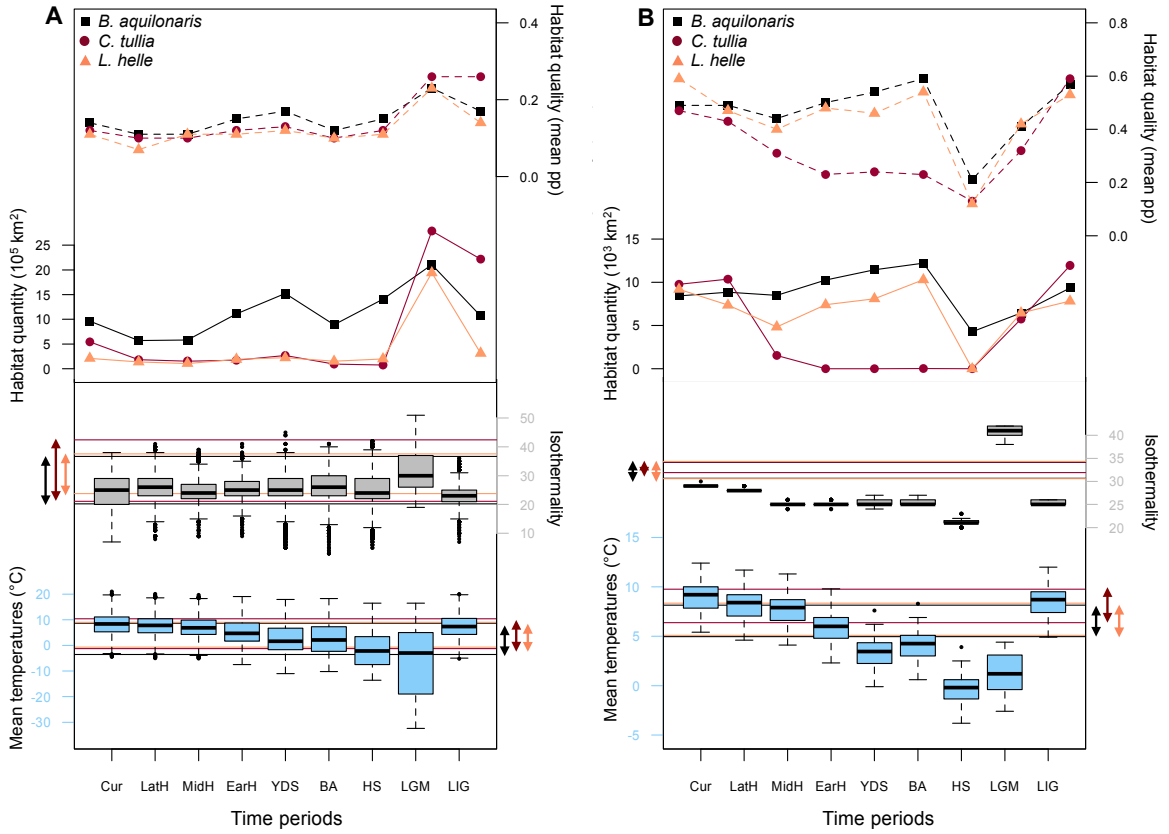

976 **Figure 6. Changes in climate suitability over time in (A) Europe and (B) the Jura massif.**
977 From top to bottom: changes in habitat quantity (full line), in habitat quality (dashed line), and
978 in climate conditions for the two temperature variables important for the current distribution of
979 species: mean annual temperature (BIO1) and isothermality (BIO3) over the nine time periods
980 considered. Cur: 1970–2000; LatH: 0.3–4.2 kya; MidH: 4.2–8.3 kya; EarH: 8.3–11.7 kya; YDS:
981 11.7–12.9 kya; BA: 12.9–14.7 kya; HS: 14.7–17.0 kya; LGM: 21 kya; LIG: 130 kya.

Tables

Table 1. Regional genetic diversity. Regions: Haut-Jura (HJ); Doubs-Drugeon valleys (DDV); plateau of Russey (RUS); and their sample sizes (N). Diversity indices: observed heterozygosity (Ho); expected heterozygosity (He); inbreeding coefficient (F_{IS}); population-specific differentiation (F_{ST}). 95% confidence intervals (CIs) based on bootstraps of the data.

Species	Region	N	Ho		He		F_{IS}		F_{ST}	
			value	95% CI	value	95% CI	value	95% CI	value	95% CI
B. aquilonaris	HJ	10	0.209	0.183-0.236	0.241	0.218-0.266	0.134	0.060-0.219	0.289	0.231-0.348
	DDV	20	0.211	0.186-0.237	0.252	0.223-0.278	0.138	0.018-0.223	0.262	0.213-0.332
	RUS	17	0.220	0.192-0.250	0.264	0.239-0.290	0.198	0.102-0.253	0.228	0.176-0.284
	All	47	0.212	0.187-0.239	0.255	0.230-0.279	0.169	0.068-0.234	0.235	0.179-0.303
C. tullia	HJ	16	0.132	0.121-0.145	0.196	0.180-0.212	0.314	0.258-0.384	0.206	0.161-0.258
	DDV	53	0.135	0.121-0.149	0.193	0.180-0.204	0.296	0.247-0.344	0.186	0.161-0.245
	RUS	18	0.142	0.131-0.154	0.219	0.205-0.233	0.377	0.325-0.413	0.078	0.049-0.128
	All	87	0.135	0.122-0.149	0.199	0.183-0.212	0.321	0.247-0.351	0.178	0.131-0.221
L. helle	HJ	69	0.137	0.121-0.151	0.157	0.143-0.172	0.140	0.081-0.197	0.201	0.155-0.276
	DDV	97	0.152	0.139-0.164	0.177	0.164-0.190	0.151	0.072-0.198	0.091	0.039-0.144
	RUS	52	0.137	0.124-0.152	0.160	0.149-0.171	0.132	0.092-0.213	0.185	0.121-0.244
	All	218	0.143	0.129-0.157	0.167	0.155-0.179	0.145	0.076-0.208	0.151	0.103-0.214

Table 2. Identification of the best divergence scenarios between regions for each species. Analysis 1 tested the period (ancient vs. recent) and the mode (during increase vs. decrease in Ne) of divergence; all synchronous. Analysis 2 tested the simultaneous divergence of the three populations or whether one population diverged first. Prior and posterior distributions of parameters are in supplementary Tables S3 and S5, respectively, and schematic representation of split times and sequence in Figure 4B.

Analysis 1. Period and factor of divergence						
Species	**Split-Exp**	**Split-1D**	**Split-2D**	**Best scenario**	**Type I error**	**Type II error**
B. aquilonaris	no tested	0.000 [0.000-0.000]	1.000 [1.000-1.000]	Recent split / Decline	0.05	0.05
C. tulla	0.000 [0.000-0.000]	0.005 [0.001-0.009]	0.999 [0.999-1.000]	Recent split / Decline	0.04	0.00 / 0.04
L. helle	0.000 [0.000-0.000]	0.000 [0.000-0.001]	0.999 [0.999-1.000]	Recent split / Decline	0.06	0.00 / 0.06
Analysis 2. Divergence sequence						
Species	**Synch-Split**	**Asynch-Split1**	**Asynch-Split2**	**Best scenario**	**Type I error**	**Type II error**
B. aquilonaris	0.000 [0.000-0.000]	0.001 [0.000-0.002]	0.999 [0.998-0.999]	Asynchronous / RUS first	0.03	0.02 / 0.01
C. tulla	0.001 [0.000-0.001]	0.000 [0.000-0.001]	0.999 [0.999-1.000]	Asynchronous / RUS first	0.08	0.08 / 0.00
L. helle	0.001 [0.000-0.001]	0.000 [0.000-0.001]	0.999 [0.999-1.000]	Asynchronous / RUS first	0.12	0.11 / 0.01

Table 3. Species climatic requirements. For each of the six bioclim variables included in SDMs, the range is given for any variable having a relative importance >10% and represents the range observed in predicted areas with high presence probability of the species (pp > ppTSS) at the European scale and in the Jura massif. BIO1: Mean annual temperature; BIO2: Mean diurnal range; BIO3: isothermality; BIO8: mean temperature of the wettest quarter; BIO12: annual precipitation; BIO15: precipitation seasonality.

Bioclim	**Relative importance**			**Range of variable Western Europe**			**Range of variable Jura massif**		
variable	*B. aquilonaris*	*C. tullia*	*L. helle*	*B. aquilonaris*	*C. tullia*	*L. helle*	*B. aquilonaris*	*C. tullia*	*L. helle*
BIO1	47%	43%	56%	-3.5 – 8.7	-1.3 – 10.4	0.7 – 9.0	5.0 – 8.2	6.4 – 9.8	5.1 – 8.4
BIO2	2%	11%	4%		4.80 – 10.37			7.84 – 8.89	
BIO3	18%	14%	23%	20.2 – 36.7	21.1 – 42.4	23.8 – 37.6	30.7 – 34.1	31.9 – 34.2	30.6 – 34.3
BIO8	21%	15%	4%	-8.8 – 16.2	-2.4 – 17.8		-1.0 – 12.7	0.0 – 12.7	
BIO12	1%	6%	2%						
BIO15	11%	11%	10%	7.8 – 48.2	7.8 – 46.8	7.0 – 51.7	7.8 – 11.2	7.8 – 12.1	8.1 – 11.8